Applied Microbiology and Biotechnology (2023) 107:7313–7330
https://doi.org/10.1007/s00253-023-12786-9

METHODS AND PROTOCOLS

Nile red-based lipid fluorometry protocol and its use for statistical optimization of lipids in oleaginous yeasts

Benjamin Ouellet[1,2] · Zacharie Morneau[1] · Ahmad M. Abdel-Mawgoud[1,2]

Received: 15 June 2023 / Revised: 6 September 2023 / Accepted: 7 September 2023 / Published online: 23 September 2023

Abstract

As lipogenic yeasts are becoming increasingly harnessed as biofactories of oleochemicals, the availability of efficient protocols for the determination and optimization of lipid titers in these organisms is necessary. In this study, we optimized a quick, reliable, and high-throughput Nile red-based lipid fluorometry protocol adapted for oleaginous yeasts and validated it using different approaches, the most important of which is using gas chromatography coupled to flame ionization detection and mass spectrometry. This protocol was applied in the optimization of the concentrations of ammonium chloride and glycerol for attaining highest lipid titers in *Rhodotorula toruloides* NRRL Y-6987 and *Yarrowia lipolytica* W29 using response surface central composite design (CCD). Results of this optimization showed that the optimal concentration of ammonium chloride and glycerol is 4 and 123 g/L achieving a C/N ratio of 57 for *R. toruloides*, whereas for *Y. lipolytica,* concentrations are 4 and 139 g/L with a C/N ratio of 61 for *Y. lipolytica*. Outside the C/N of 33 to 74 and 45 to 75, respectively, for *R. toruloides* and *Y. lipolytica*, lipid productions decrease by more than 10%. The developed regression models and response surface plots show the importance of the careful selection of C/N ratio to attain maximal lipid production.

Key points

- *Nile red (NR)-based lipid fluorometry is efficient, rapid, cheap, high-throughput.*
- *NR-based lipid fluorometry can be well used for large-scale experiments like DoE.*
- *Optimal molar C/N ratio for maximum lipid production in lipogenic yeasts is ~60.*

Keywords Central composite design · Oleaginous yeasts · Nile red · *Yarrowia lipolytica* · *Rhodotorula toruloides* · Lipid fluorometry

Introduction

Oleaginous yeasts are microorganisms that can accumulate lipids to more than 20% of their dry cell mass (Papanikolaou and Aggelis 2011a; Ratledge and Wynn 2002). They have garnered attention for their promising potential as low-cost biofactories for the production of oleochemicals like biofuels, dietary supplements, and other lipid-based chemicals (Abdel-Mawgoud et al. 2018). Furthermore, lipogenic yeasts can efficiently utilize a vast variety of cheap carbon sources (Dobrowolski et al. 2019), one of which is glycerol that costs 0.1–0.75 US$ per kg (Quispe et al. 2013), a by-product of the biodiesel industry, and that can replace more costly carbon sources like glucose (da Silva et al. 2009).

Yarrowia lipolytica and *Rhodotorula toruloides* are two of the best studied oleaginous yeasts, accumulating high lipid titers reaching about 40% (Nicaud 2012) and 70% (Johns et al. 2016) of their dry cell weights, respectively. Although more knowledge (Abdel-Mawgoud et al. 2018) and genetic engineering tools (Abdel-Mawgoud and Stephanopoulos 2020; Ouellet and Abdel-Mawgoud 2023) are available for *Y. lipolytica*, the high lipid titers of *R. toruloides* and its co-production of carotenoids with

Benjamin Ouellet and Zacharie Morneau are the co-first authors.

✉ Ahmad M. Abdel-Mawgoud
ahmad.saleh@bcm.ulaval.ca

[1] Institute of Integrative Biology and Systems, Laval University, Pavillon Charles-Eugène-Marchand, 1030 Ave. de la Médecine,, QC, QC G1V 0A6, Canada

[2] Department of Biochemistry, Microbiology and Bioinformatics, Faculty of Science and Engineering, Laval University, 1045 Ave. de la Médecine, QC, Quebec G1V 0A6, Canada

therapeutic and nutritional potential are attracting attention towards this latter yeast (Johns et al. 2016).

Cost-effective production of lipids by oleaginous yeasts using cheap carbon and nitrogen sources is highly desired to support economical large-scale lipid production processes (Kitcha and Cheirsilp 2011). Therefore, many studies explored the optimal concentration of carbon and nitrogen sources to maximize lipid production (Kitcha and Cheirsilp 2011) being the important elements triggering lipid accumulation in oleaginous yeasts.

On the biochemical level, oleaginous yeasts have in common a high metabolic flux of acetyl-CoA, the primary building block of lipids. This high acetyl-CoA flux is induced by limitation of nitrogen and together with an excess of carbon contents in the culture medium (Papanikolaou and Aggelis 2011a; Ratledge and Wynn 2002). When nitrogen is limited in the medium, the cell activates a mechanism to scavenge nitrogen by the deamination of adenosine monophosphate (AMP) via the AMP deaminase leading to a sharp reduction of AMP and subsequently sharp reduction in the activity of isocitrate dehydrogenase (ICDH), as AMP is an activator of ICDH (Ratledge and Wynn 2002) (Fig. 1). This leads to the accumulation of citrate in the mitochondria that is then exported to the cytoplasm by the malate/citrate antiport shuttle (Abdel-Mawgoud et al. 2018; Ratledge and Wynn 2002) (Fig. 1). Cytosolic citrate is converted into oxaloacetate and acetyl-CoA by the action of ATP:citrate lyase (ACLY) which acts as the key supplier of cytosolic acetyl-CoA required

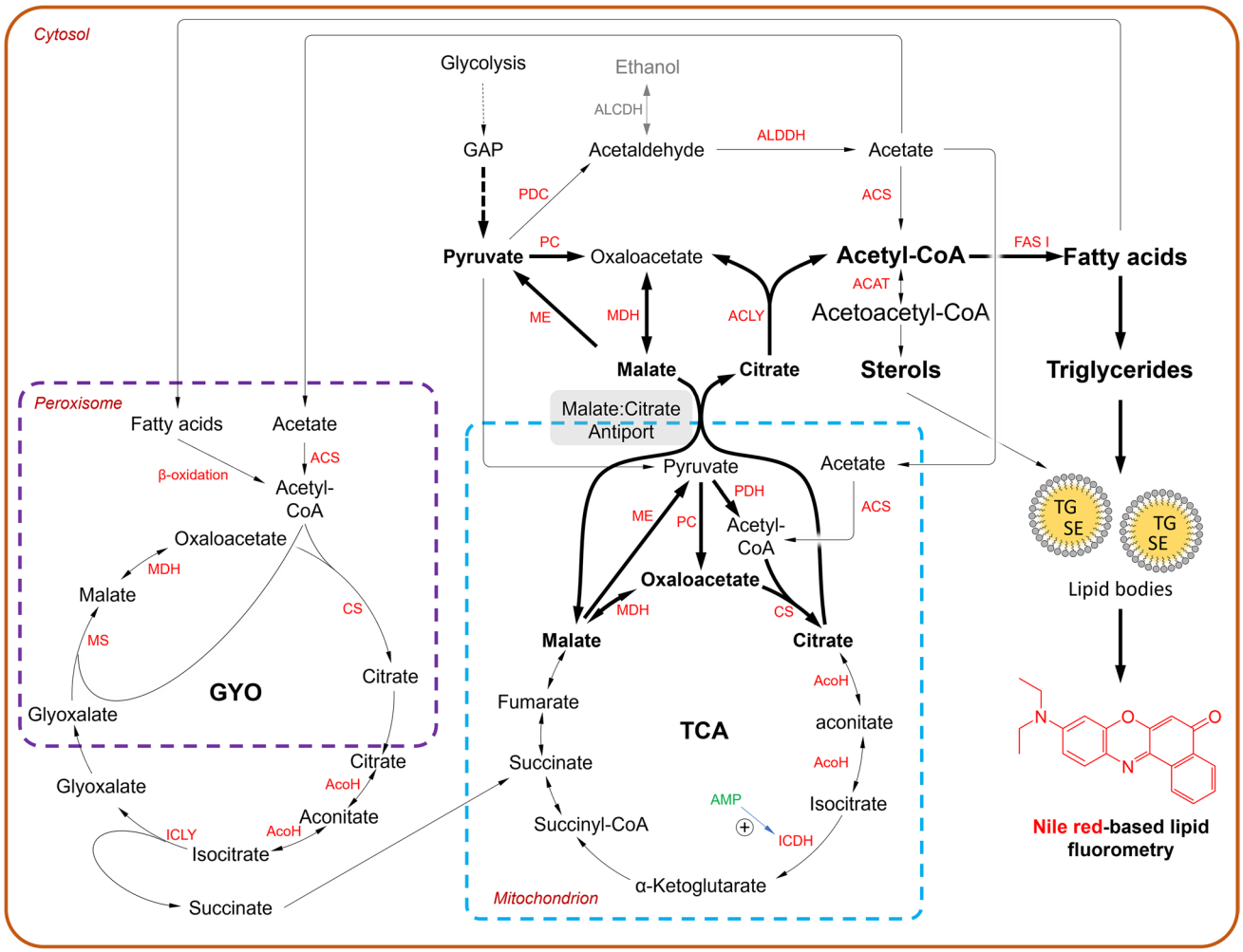

Fig. 1 Pathways involved in lipogenesis in oleaginous yeasts. ACLY, ATP-citrate lyase; AcoH, aconitate hydratase; ACS, acetyl-CoA synthase; ALDDH, aldehyde dehydrogenase; ALCDH, alcohol dehydrogenase; CS, citrate synthase; FAS I, fatty acid synthase I; GAP, glyceraldehyde phosphate; GYO, glyoxylate cycle; ICDH, isocitrate dehydrogenase; ICLY, isocitrate lyase; MDH, malate dehydrogenase; ME, malic enzyme; MS, malate synthase; PC, pyruvate carboxylase; PDC, pyruvate decarboxylase; PDH, pyruvate dehydrogenase; TCA, tricarboxylic acid cycle; TG, triglycerides; SE, sterol esters. Thick arrows represent reaction of high fluxes in oleaginous yeasts. The chemical structure (red) is of Nile red dye used for lipid fluorometry. The biochemical chart is inspired from multiple previous works (Abdel-Mawgoud et al. 2018; Hildyard and Halestrap 2003; Nielsen 2014; Ratledge 1997; Ratledge and Wynn 2002)

for lipogenesis (Abdel-Mawgoud et al. 2018; Ratledge and Wynn 2002; Zhang et al. 2016). Lipids, triglycerides (TG), formed during lipogenesis are stored in highly hydrophobic cores of lipid bodies bound by a phospholipid monolayer carrying membrane-bound proteins, like perilipin (Henne et al. 2018) (Fig. 1).

Lipid quantities in oleaginous yeasts vary according to culture conditions and genetic backgrounds. Investigation of factors affecting lipid production requires large-scale studies, like using design of experiment (DoE), which are experimentally intensive and necessitate rapid, high-throughput, and efficient methods for lipid quantification; these latter are unfortunately lacking.

Usually, lipids are quantified using chromatographic methods, like thin layer chromatography (TLC) and gas chromatography coupled to flame ionization detection (GC/FID) (Blazeck et al. 2014; Pomraning et al. 2015). While these methods are fairly precise, selective, and sensitive, they require laborious sample preparation; are costly, time consuming, and mostly low-throughput; and are generally unable to estimate all lipids present in the sample; i.e., they can only target known lipids, unless an exhaustive lipidomic analysis is made which is to-date experimentally unattainable.

Nile red (NR)-based lipid fluorometry is instead a promising method that can be developed for large-scale lipid estimation in oleaginous organisms (Kimura et al. 2004; Miranda et al. 2020; Orr and Rehmann 2015), as it is cheap and can be directly applied on cells without prior treatment. NR is more commonly used as a lipophilic fluorescent dye in microscopy for visualization of lipid droplets (Blazeck et al. 2014; Greenspan and Fowler 1985), yet it has been scarcely used for precise lipid quantification (Kimura et al. 2004; Miranda et al. 2020; Orr and Rehmann 2015). This is because current NR-based lipid fluorometry methods lack sufficient optimization and necessary standardization and validation. These problems limited the use of NR-fluorometry in precise and high-throughput lipid quantification in large-scale experiments.

In this study, we developed an optimized and standardized NR-based lipid quantification method that we then applied for optimization of medium components using DoE. This novel method was validated using GC-FID/MS analysis and was subsequently used for lipid estimations in the optimization of carbon and nitrogen source concentrations for maximizing lipid production in *R. toruloides* and *Yarrowia lipolytica* using DoE.

Material and methods

Strains and growth conditions

The strains used in this study were *Yarrowia lipolytica* W29 (ATCC 20460), *Rhodotorula toruloides* (NRRL Y-6987), *Saccharomyces cerevisiae* FY4 (MatA), *Escherichia coli* DH5α (Invitrogen #18265017), and *Escherichia coli* BL21 (NEB #C2530H). Yeast Peptone Dextrose Broth (YPD, Bio Basic, Canada) was used for preparation of biomass that was used to inoculate Yeast Nitrogen Base media at an initial optical density at 600 nm (OD_{600}) of 0.1. Yeast Nitrogen Base (YNB, Bio Basic, Canada), free of amino acids and ammonium sulfate that was supplemented with glycerol (Fisher scientific) and ammonium chloride (Bio Basic, Canada), was used for lipid production. Unless otherwise mentioned, the composition of the YNB lipogenic media was 1.7 g/L YNB, 86.1 g/L glycerol, 3 g/L NH_4Cl, and 25 mM sodium phosphate buffer (pH 6.8). This medium formulation achieves a molar carbon-to-nitrogen (C/N) ratio of 50. The OD_{600} of the cultures was measured using a 96-well plate reader (Multiskan, Thermo Fisher Scientific).

Lipid quantification by Nile red fluorescence

As per the protocol developed in this study, cultures grown in YNB were diluted to a final OD_{600} between 2 and 6 at a final volume of 500 µL in 25 mM sodium phosphate buffer (pH 6.8) in 1.5-mL microtubes. Then, 50 µL of a Nile red dye solution (100 µg/mL, TCI America, in acetone) was added at a final NR concentration of 10 µg/mL. The hermetically closed and light protected microtubes were incubated at 60 °C for 30 min during which the tubes were agitated every 5 min on average. After incubation, 200 µL was pipetted from each microtube and transferred into wells of an all-opaque, white 96-well plate and fluorescence was measured using a fluorescence plate reader (Fluoroskan, Thermo Fisher Scientific) equipped with a pair of excitation and emission filters at 544 nm and 678 nm, respectively. Fluorescence values were corrected for the intrinsic fluorescence of NR where cell samples were replaced with equivalent volume of 25 mM sodium phosphate buffer (SPB, pH 6.8) alone. In addition, corrections against cell autofluorescence were made where 50 µL of pure acetone was added in replacement to the NR solution. Recorded relative fluorescence units (RFU) were then corrected to RFU/L of original liquid culture.

For high-throughput NR-based total lipid quantification, we further developed a protocol in this study where both cell staining and fluorescence measurement are conducted in one step in all-opaque, white 96-well plate. In our setup, white plates resulted in 5 times higher fluorescence signals than those obtained in black plates (data not shown). Two hundred microliters of diluted cells in 25 mM SPB pH 6.8 between 2 and 6 OD_{600} was loaded onto 96-well plates. Twenty microliters of NR (100 µg/

mL in acetone) was distributed into each well, for a final concentration of 10 µg/mL, which were sealed with adhesive microplate films (Sarstedt) and incubated at 60 °C while shaking for 30 min in the dark. Plate fluorescence was then measured with controls as mentioned above.

Dry biomass measurement

Aliquots of 1.5 mL of liquid cultures were pipetted into preweighed 1.5-mL microtubes (Axygen, Corning, USA) that were centrifuged for 5 min at maximum speed (22,000*g*) after which the supernatant was discarded. Cell pellets were washed twice with a volume of 25 mM SPB and dried at 60 °C for at least 24 h or until a constant weight was reached and then weighed to calculate dry cell masses.

Lipid analysis by GC-FID

Cell lipids were derived into fatty acid methyl esters (FAME) using a modified in situ transesterification method developed by van Wychen et al. (2016). An amount of liquid cell culture equivalent to 5,000 OD·µL was transferred to 1.5-mL GC vials. Cells were then pelleted, washed twice with 1 mL of 25 mM SPB, and subsequently dried at 60°C for at least 4 h. A volume of 10 µL of C13:0 methyl ester (10 mg/mL; Fisher Scientific, Canada) was added as an internal standard. A volume of 200 µL of chloroform:methanol 2:1 v/v (Fisher Scientific, Canada) and 300 µL of 0.6 M HCl in methanol (Fisher Scientific, Canada) was added to vials which were then sealed with screw caps, mixed, and incubated at 85°C for 1 h. Vials were left to cool down to room temperature; then, FAMEs were extracted by adding 1 mL of high-performance liquid chromatography (HPLC) grade hexane (Fisher Scientific, Canada) and vortexing for 10 s. Phase separation was induced by centrifuged at 22,000*g* for 10 min. The hexane layer was recovered and transferred into a new 1.5-mL GC vial for analysis by GC.

A volume of 1 µL was injected under a split ratio of 1:10 into a GC-FID (Trace 1300 Gaz chromatograph system, Thermo Fisher Scientific) equipped with a TraceGOLD TG-5MT metal capillary column (ID of 0.25 mm, length of 30 m, film thickness of 0.25 µm composed of (5%-phenyl)-methylpolysiloxane; Thermo Fisher Scientific). Elution and oven settings were set as following: inlet temperature = 280 °C, carrier gas (helium) flow = 1 mL/min, oven = 50 °C for 1 min, increased by 25 °C/min to 180 °C, hold 2 min, increased by 0.5 °C/min to 190 °C, increased by 10 °C/min to 350 °C, increased by 25 °C/min to 380 °C, and hold 2 min. Detection settings were the following: FID temperature = 380 °C, hydrogen flow = 40 mL, air = 450 mL, and makeup gas (nitrogen) = 30 mL. All GC gases were 99.999% purity (Linde, Canada).

Calibration curves for lipid quantification were obtained with a 30-component FAME standard C8-24 (461-C, Nu-Chek-Prep, USA) that was complemented with C2:0 acetic acid (Thermo Fisher Scientific); C4:0, butanoic acid (Sigma-Aldrich); C5:0, pentanoic acid (Thermo Fisher Scientific); C6:0, hexanoic acid (Sigma-Aldrich);, and C7:0, heptanoic acid (TCI) standards derived in FAMEs. The identity of corresponding peaks of these standards was further confirmed by GC-MS (data not shown). The list of standard FAMEs and their retention times are listed in supplementary information (Table S1), and a corresponding GC-FID chromatogram is shown (Figure S1).

Full factorial central composite design for medium optimization

To determine the optimal concentration of glycerol and NH_4Cl (test variables, factors) in YNB medium for maximal lipid production by *Y. lipolytica* W29 and *R. toruloides* NRRL Y6987, we employed a 2^2 full factorial central composite design with the following setup: 2 factors (test variables, glycerol and ammonium chloride concentrations), 2 levels (concentrations, not including the central or star points), star point (α) value = 1.41421, 3 replicates, organized in 1 block. The coded values, $-\alpha$, -1, 0, $+1$, and $+\alpha$, corresponded to the following actual values of ammonium chloride (X_1, g/L): 4, 5.2, 8, 10.8, and 12 g/L, respectively. For glycerol, these coded values corresponded to actual values of glycerol (X_2, /L): 50, 72, 125, 178, and 200 g/L, respectively. This made a total number of 39 runs, composed of 12 cube points, 15 center points (in cube), and 12 axial (star) points (with no center points in axial runs) (Table 1). The dependent variables (responses) selected for this study were lipid titers in NR fluorescence units (Y_1, RFU/L) and gas chromatography (Y_2, mg/L) and dry biomass (Y_3, g/L). Minitab software (version 17.1.0) was used to generate run designs, to perform statistical analyses (ANOVA and Student *t*-test), to generate regression models, and to predict optimal values of test variables from the generated regression model. The best model was generated with a stepwise regression method, involving both forward selection and backward elimination of terms with an $\alpha = 0.05$, while removing the constraint of respecting a hierarchical model.

Results

Optimization of the Nile red-based lipid quantification method

First, we wanted to determine the range of linearity of NR fluorescence intensity as a function of cell density. Cells of *Y. lipolytica* and *R. toruloides* were collected

Table 1 Central composite design matrix of coded and actual values of factors along with the experimental lipid titers for medium optimization for *R. toruloides* Y-6987

Run	Coded values		Actual values (g/L)		Responses		
	X_1: NH_4Cl	X_2: glycerol	X_1: NH_4Cl	X_2: glycerol	Y_1: lipid titer (RFU/L)	Y_2: lipid titer (mg/L)	Y_3: dry biomass (g/L)
1	−1	−1	5.2	72	3,648,417	1,039	11.3
2	1	−1	10.8	72	3,828,417	864	12.1
3	−1	1	5.2	178	2,501,917	630	16.5
4	1	1	10.8	178	2,322,417	567	15.3
5	−1.41421	0	4	125	4,437,417	791	16.1
6	1.41421	0	12	125	3,435,417	601	14.0
7	0	−1.41421	8	50	2,929,917	859	10.0
8	0	1.41421	8	200	2,632,417	456	15.4
9	0	0	8	125	4,065,917	799	16.1
10	0	0	8	125	4,227,417	861	14.3
11	0	0	8	125	4,362,417	801	14.7
12	0	0	8	125	4,382,417	786	14.7
13	0	0	8	125	3,813,417	781	14.1
14	−1	−1	5.2	72	3,651,417	1,040	12.3
15	1	−1	10.8	72	3,402,417	735	11.9
16	−1	1	5.2	178	3,213,917	554	18.7
17	1	1	10.8	178	2,667,917	472	15.3
18	−1.41421	0	4	125	4,307,417	936	15.5
19	1.41421	0	12	125	3,208,917	569	12.6
20	0	−1.41421	8	50	3,265,417	852	9.3
21	0	1.41421	8	200	2,440,917	456	15.5
22	0	0	8	125	4,066,417	792	14.8
23	0	0	8	125	4,115,917	781	12.5
24	0	0	8	125	3,708,417	793	13.9
25	0	0	8	125	3,935,417	776	15.3
26	0	0	8	125	3,752,917	746	14.5
27	−1	−1	5.2	72	3,930,417	962	13.3
28	1	−1	10.8	72	3,859,417	696	11.0
29	−1	1	5.2	178	3,314,417	560	16.0
30	1	1	10.8	178	2,572,917	369	14.3
31	−1.41421	0	4	125	5,132,417	1,073	16.3
32	1.41421	0	12	125	3,618,917	523	14.5
33	0	−1.41421	8	50	3,596,417	696	10.5
34	0	1.41421	8	200	2,916,917	419	16.5
35	0	0	8	125	3,754,917	723	14.3
36	0	0	8	125	3,852,417	727	14.9
37	0	0	8	125	3,961,917	747	15.4
38	0	0	8	125	3,819,917	671	14.6
39	0	0	8	125	3,759,417	740	14.2

from culture grown in liquid YNB medium, serially diluted to different 600 nm optical densities (OD_{600}), and stained with NR, and their fluorescence intensities were measured (Fig. 2).

For both yeasts, the ranges of linearity of fluorescence values were close to each other, which is at a range of OD_{600} from 2 to 8 for *Y. lipolytica* (Fig. 2B) and at a range of OD_{600} from 2 to 6 in *R. toruloides* (Fig. 2D). Accordingly, in subsequent experiments no matter the nature of the studied yeast, we decided to dilute cultures to the common linear range, which is to an OD_{600} between 2 and 6 for NR staining.

Second, we thought that NR solubility and diffusion across membranes and within lipid bodies were limiting and could be enhanced by heating the NR dye with cell suspensions so that more NR molecules accumulate into

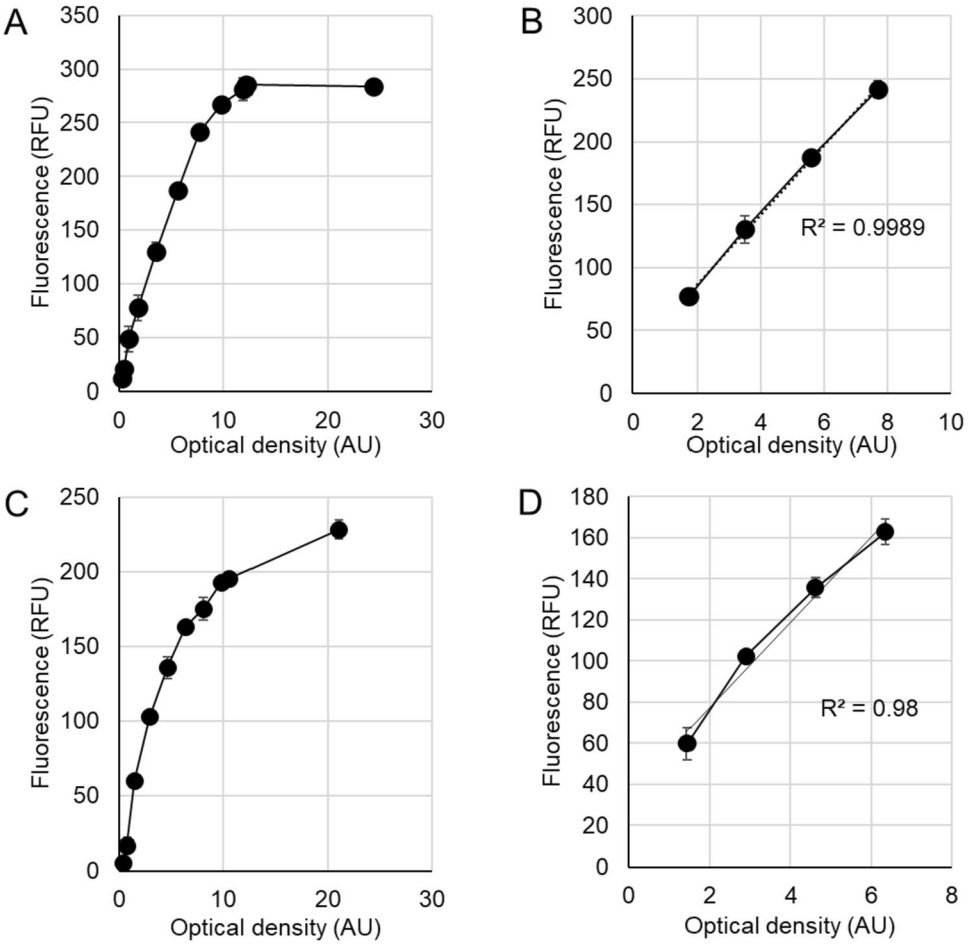

Fig. 2 Dynamic range of Nile red-based fluorometry of lipids as a function of optical density in oleaginous yeasts. Fluorescence recorded at all tested optical densities of **A** *Y. lipolytica* W29 and **C** *R. toruloides* Y-9687 cells. The dynamic range of Nile red-based fluorometry of lipids and the correlation coefficient R^2 are shown for **B** *Y. lipolytica* W29 and **D** *R. toruloides* Y-6987. Cells were harvested from a 2-day-old culture cultivated in YNB-glycerol-NH_4Cl, C/N ratio: 50. RFU, relative fluorescence units; AU, absorbance units at 600 nm. The mean and the standard deviation are for data obtained from biological triplicate experiments

lipid bodies leading to higher fluorescence signals. To validate this hypothesis, cell suspensions were stained with NR and then incubated at different temperatures, namely, at 25 °C, 37 °C, 50 °C, and 60 °C, for 30 min, and fluorescence values were compared.

Indeed, increasing NR staining temperature from 25 to 60 °C increased the fluorescence signal by more than 3- and 10-fold in *Y. lipolytica* and *R. toruloides*, respectively (Fig. 3A), whereas a less than 0.5-fold increase was observed when going from 25 to 37 °C (Fig. 3A). Therefore, we decided to incubate cells at 60 °C during NR staining in subsequent experiments.

We then sought to determine the optimal incubation time at the selected staining temperature, 60 °C, for NR staining of oleaginous yeast. To do so, we incubated cells with NR dye at 60 °C for different periods ranging from 5 to 60 min (Fig. 3B).

Results show that the fluorescence signals increased nearly linearly as a function of incubation time in the range of 5 to 30 min where fluorescence signals increased 2- to 3-fold; however, a plateau was reached after 30 min of staining time or only a slight signal increase could be observed after 60 min compared to 30 min of incubation (Fig. 3B). Accordingly, we selected 30 min as the optimal incubation time in subsequent NR staining.

Using Nile red-based lipid fluorometry to determine lipogenicity of microorganisms

We wanted to examine the capacity of our NR staining protocol in distinguishing lipogenic from non-lipogenic microorganisms by comparing their fluorescence signals normalized to biomass (RFU/g). To do so, we compared biomass normalized NR fluorescence values in known oleaginous and non-oleaginous microorganisms.

As expected, oleaginous species, namely, *R. toruloides* Y-6987 and *Y. lipolytica* W29, showed 2–3 times higher RFU/g ratio than non-oleaginous organisms, namely, *Saccharomyces cerevisiae* FY4 MATa, *Escherichia coli* BL21, and *Escherichia coli* DH5*α* (Fig. 3C). Accordingly, we suggest that the cutoff for a yeast to be classified as lipogenic is to have at least 3 times the specific fluorescence

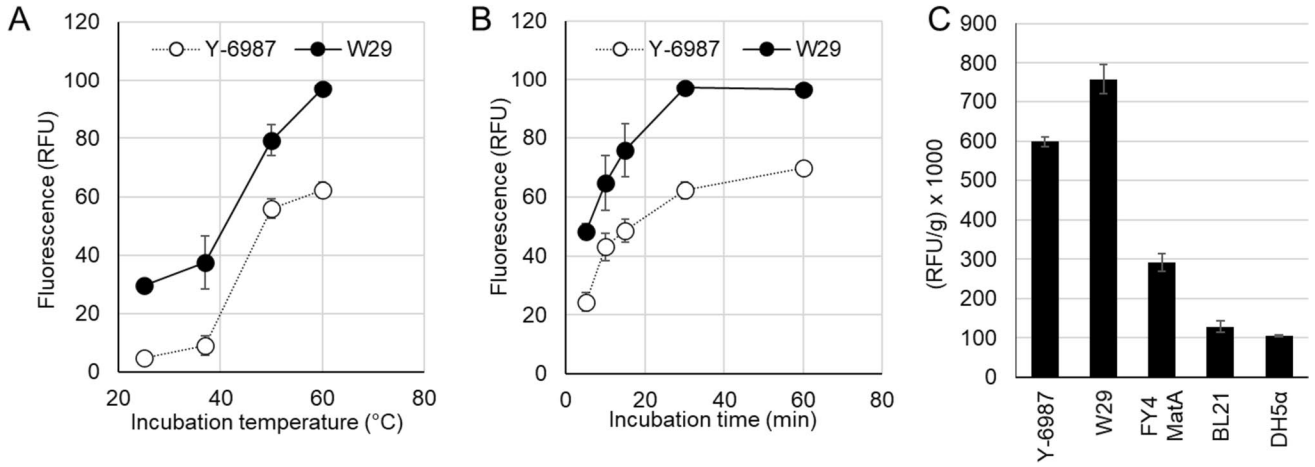

Fig. 3 Effect of NR staining temperature and time on fluorescence intensity and the use of these conditions for the determination of lipogenicity of microorganisms. Fluorescence intensity was recorded for NR staining of lipid bodies of *Y. lipolytica W29* and *R. toruloides* Y-6987 after incubation **A** at different temperatures for 30 min and **B** at different staining times while incubating at 60 °C. **C** Specific lipid production (RFU/g biomass) was determined for the lipogenic yeasts, *R. toruloides* Y-6987 and *Y. lipolytica* W29, the non-lipogenic yeast, *S. cerevisiae* FY4, and the non-lipogenic bacteria, *E. coli* BL21 and *E. coli* DH5*α*. Cells were cultivated in YNB-glycerol-NH_4Cl, C/N ratio: 50. They were harvested after 2 days of growth for **A** and **B** yet after 3 days for **C**. The mean and the standard deviation are of data obtained from triplicate experiments

signal (RFU/g dry biomass) of that of *E. coli* or 2 times that of *S. cerevisiae* using our Nile red-based lipid fluorometry protocol.

Kinetics of lipid accumulation in two lipogenic yeasts

Using the developed NR-based lipid fluorometry, the kinetics of lipid accumulation throughout the growth curve were studied in the two oleaginous yeasts (Fig. 4). *Y. lipolytica* reached its highest absolute lipid titer on the 3rd day of growth, whereas *R. toruloides* achieved comparable lipid titers only after 7 to 8 days of incubation (Fig. 4A). This might be attributed to the slower growth of *R. toruloides* which achieved higher net growth on days 7 and 8 than that of *Y. lipolytica* (Fig. 4A). Interestingly, however, both yeasts showed comparable specific lipid productivity (RFU/g dry biomass, lipid content) throughout the growth curve, with a peak of lipid productivity occurring on the 3rd day of growth for both yeasts (Fig. 4B).

Since the peak of specific lipid productivity is on the 3rd day of growth in both yeasts, 3 days of incubation was selected as the time to harvest cells in subsequent experiments.

GC-FID validation of Nile red-based lipid fluorometry

We then proceeded into the validation of the lipid quantification capacity of Nile red-based lipid fluorometry by GC-FID. To do so, we determined the lipid titers in different cell masses by NR-based lipid fluorometry and by GC-FID. A serial dilution of 3-day-old cell suspensions of *Y. lipolytica* and *R. toruloides* was prepared at OD_{600} from 2 to 6. From each dilution, 1 mL was collected for GC-FID lipid analysis in addition to NR-based lipid fluorometry. Our results demonstrate a strong correlation (R^2 of 0.9718 and 0.9824) between lipid titers obtained by GC-FID and our NR-based lipid fluorometry in both *R. toruloides* and *Y. lipolytica* (Fig. 4C), thus providing a strong indication of the validity of our developed NR-based lipid fluorometry for precise lipid quantification.

Application of NR-based lipid fluorometry in high-throughput DoE

We wanted to further validate and apply the NR-based lipid fluorometry in high-throughput experiments like DoE. We thus decided to use this lipid quantification protocol in DoE for the optimization carbon and nitrogen sources for maximal lipid production in the two studied yeasts.

Given the cheap prices of glycerol that are around 0.1 and 0.75 US$ per kg for crude and refined glycerol, respectively (Quispe et al. 2013), and around 0.4–0.75 US$ per kg for ammonium chloride (according to Alibaba.com), we decided to optimize them as the carbon and nitrogen sources, respectively, in the YNB medium aiming at maximal lipid production by *Y. lipolytica* W29 and *R. toruloides* Y-6987. For each run of the central composite design (CCD), we measured lipid titers using both NR (RFU/L)

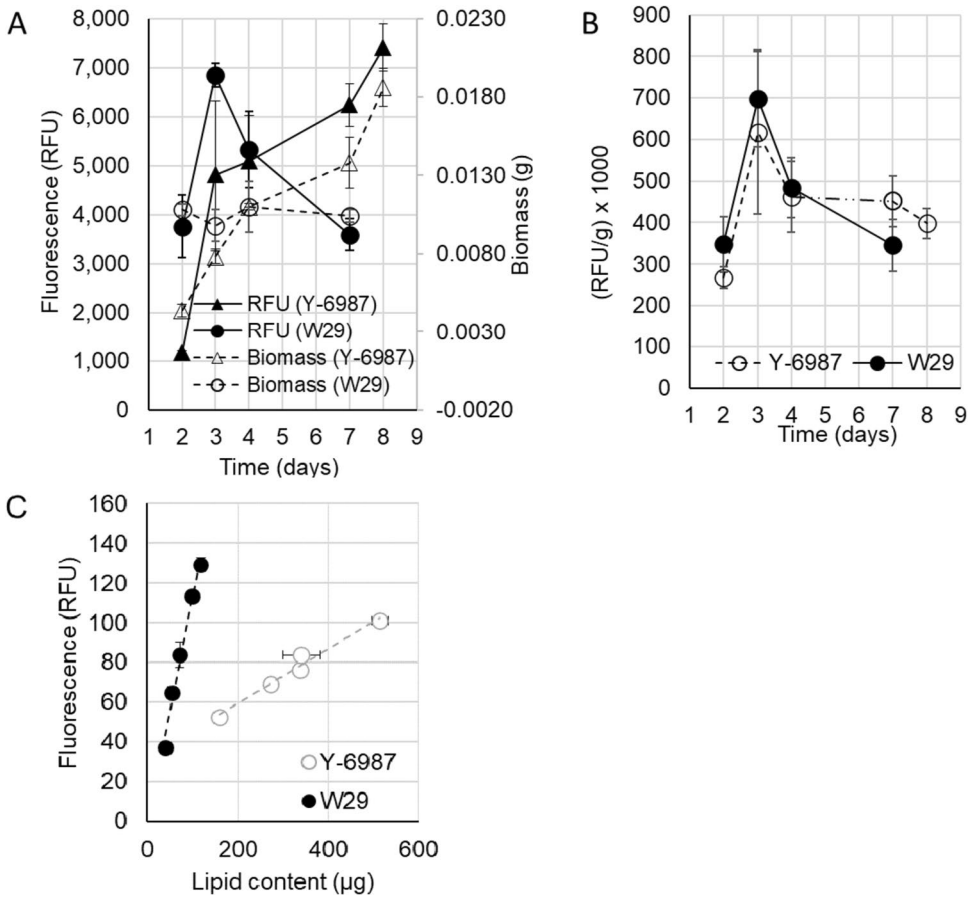

Fig. 4 Kinetics of lipid accumulation in two lipogenic yeasts as quantified by Nile red-based fluorometry. **A** Absolute lipid titers across growth curve as measured by Nile red fluorescence (RFU). **B** Specific lipid productivity as measured by Nile red fluorescence over dry cell weight (RFU/g). Y-6987, *R. toruloides* Y-6987; W29, *Y. lipolytica* W29. **C** Nile red fluorescence (RFU) in correlation with lipid content (µg) of *R. toruloides* Y-6987 and *Y. lipolytica* W29 as measured by GC-FID with regression coefficient, R^2, of 0.9718 and 0.9824, respectively. The mean and the standard deviation are from data obtained from 3 biological replicate experiments

and GC-FID (mg/L) and dry biomass (g/L) as the dependent variables (responses), which are tabulated together with the CCD matrix in Table 1 and Table 2.

A full quadratic model was used to fit the obtained data. The analysis of variance (ANOVA) of the quadratic models for lipid titers Y_1 (RFU/L by NR) and Y_2 (mg/L by GC-FID) as well as dry biomass Y_3 (g/L) is represented in the ANOVA tables (Tables 3 and 4), followed by the respective regression equations of the models (Eqs. 1, 2, 3, 4, 5, and 6). The lipid titer (Y_1, RFU/L by NR; Y_2, mg/L by GC-FID) and dry biomass (Y_3, g/L) equations of the regression models are presented for *R. toruloides* (Eqs. 1, 2, and 3) and *Y. lipolytica* (Eqs. 4, 5, and 6), as a function of ammonium chloride (X_1) and glycerol (X_2) concentrations (g/L).

$$Y_{1,\mathrm{Rhoto}} = 1098512 + 65885\,(X_1) + 53767\,(X_2) - 198.6\,(X_2)^2 - 1310\,(X_1)\,(X_2) \quad (1)$$

$$Y_{2,\mathrm{Rhoto}} = 1073 - 39.41\,(X_1) + 3.03\,(X_2) - 0.02379\,(X_2)^2 \quad (2)$$

$$Y_{3,\mathrm{Rhoto}} = 7.36 - 0.2627\,(X_2) + 0.1121\,(X_2) - 0.000294\,(X_2)^2 \quad (3)$$

$$Y_{1,\mathrm{Yali}} = -1750139 - 198454\,(X_1) + 92584\,(X_2) - 331.5\,(X_2)^2 \quad (4)$$

$$Y_{2,\mathrm{Yali}} = -570 + 326.2\,(X_1) + 12.675\,(X_2) - 14.92\,(X_1)^2 - 0.02869\,(X_2)^2 - 0.8726\,(X_1)\,(X_2) \quad (5)$$

$$Y_{3,\mathrm{Yali}} = 5.967 + 0.2179\,(X_1) - 0.04008\,(X_2) - 0.000111\,(X_2)^2 - 0.002712\,(X_1)\,(X_2) \quad (6)$$

The ANOVA and model fitness terms of the lipid titer by NR and GC and dry biomass models for *R. toruloides* ($Y_{1,\mathrm{Rhoto}}$, $Y_{2,\mathrm{Rhoto}}$, and $Y_{3,\mathrm{Rhoto}}$) and *Y. lipolytica* ($Y_{1,\mathrm{Yali}}$, $Y_{2,\mathrm{Yali}}$, and $Y_{3,\mathrm{Yali}}$) were associated with *P*-values of 0.000. These models were also associated with insignificant ($> \alpha = 0.05$) lack-of-fit (LOF) with *P*-values of 0.211, 0.097, and 0.558, for $Y_{1,\mathrm{Toro}}$, $Y_{2,\mathrm{Toro}}$, and $Y_{3,\mathrm{Toro}}$, respectively (Table 3), and of 0.265, 0.068, and 0.261, for $Y_{1,\mathrm{Yali}}$, $Y_{2,\mathrm{Yali}}$, and $Y_{3,\mathrm{Yali}}$, respectively (Table 4), indicating that the regression models accurately represent the data in the experimental space of tested concentrations. Although still insignificant ($> \alpha = 0.05$), *P*-values of LOF of Y_2 models generated from GC-FID are closer to 0.05 (0.097 and 0.068 in *R. toruloides* and *Y. lipolytica*, respectively) compared to those of Y_1 models

Table 2 Central composite design matrix of coded and actual values of factors along with the experimental lipid titers for medium optimization for *Y. lipolytica* W29

Run	Coded values		Actual values (g/L)		Responses		
	X_1: NH_4Cl	X_2: glycerol	X_1: NH_4Cl	X_2: glycerol	Y_1: lipid titer (RFU/L)	Y_2: lipid titer (mg/L)	Y_3: dry biomass (g/L)
1	−1	−1	5.2	72	2,275,200	1,171	8.1
2	1	−1	10.8	72	1,131,100	1,281	9.1
3	−1	1	5.2	178	2,333,800	1,291	7.7
4	1	1	10.8	178	2,095,600	873	7.0
5	−1.41421	0	4	125	3,778,000	1,640	9.4
6	1.41421	0	12	125	2,278,900	945	7.8
7	0	−1.41421	8	50	1,090,450	1,286	8.0
8	0	1.41421	8	200	2,251,050	900	7.1
9	0	0	8	125	3,160,500	1,369	8.3
10	0	0	8	125	3,012,200	1,368	8.4
11	0	0	8	125	3,548,200	1,373	8.5
12	0	0	8	125	3,033,900	1,309	8.1
13	0	0	8	125	2,955,600	1,225	8.4
14	−1	−1	5.2	72	2,104,500	1,040	8.5
15	1	−1	10.8	72	1,289,400	1,300	8.4
16	−1	1	5.2	178	2,881,900	1,251	8.1
17	1	1	10.8	178	2,079,650	935	6.6
18	−1.41421	0	4	125	4,092,050	1,621	9.7
19	1.41421	0	12	125	2,505,200	953	7.6
20	0	−1.41421	8	50	1,160,250	1,283	7.9
21	0	1.41421	8	200	2,332,700	928	7.1
22	0	0	8	125	3,222,250	1,413	8.0
23	0	0	8	125	3,183,300	1,394	8.4
24	0	0	8	125	2,614,050	1,337	8.6
25	0	0	8	125	2,501,700	1,335	8.1
26	0	0	8	125	3,144,100	1,301	8.1
27	−1	−1	5.2	72	1,839,400	1,145	8.3
28	1	−1	10.8	72	1,108,450	1,333	8.1
29	−1	1	5.2	178	2,682,800	1,259	7.1
30	1	1	10.8	178	1,992,150	866	7.1
31	−1.41421	0	4	125	4,009,400	1,567	9.1
32	1.41421	0	12	125	2,442,450	992	7.9
33	0	−1.41421	8	50	676,650	1,323	8.1
34	0	1.41421	8	200	2,103,050	1,037	6.5
35	0	0	8	125	3,302,700	1,309	8.3
36	0	0	8	125	3,342,000	1,327	8.2
37	0	0	8	125	3,161,550	1,359	7.8
38	0	0	8	125	3,126,800	1,330	8.0
39	0	0	8	125	3,834,100	1,242	8.5
40	−1	−1	5.2	72	1,839,400	1,145	8.3
41	−1	−1	5.2	72	1,418,950	1,117	8.1
42	1	−1	10.8	72	506,900	1,345	8.6
43	1	−1	10.8	72	1,108,450	1,333	8.2
44	−1	1	5.2	178	2,682,800	1,259	7.1
45	−1	1	5.2	178	1,901,400	1,127	7.3
46	1	1	10.8	178	1,988,700	884	7.0
47	1	1	10.8	178	2,164,350	942	6.4
48	−1.41421	0	4	125	4,168,450	1,836	9.1
49	−1.41421	0	4	125	3,604,150	1,799	9.7

Table 2 (continued)

Run	Coded values		Actual values (g/L)		Responses		
	X_1: NH_4Cl	X_2: glycerol	X_1: NH_4Cl	X_2: glycerol	Y_1: lipid titer (RFU/L)	Y_2: lipid titer (mg/L)	Y_3: dry biomass (g/L)
50	1.41421	0	12	125	1,486,900	1,066	8
51	1.41421	0	12	125	2,442,450	992	7.9
52	0	−1.41421	8	50	1,160,250	1,283	7.9
53	0	−1.41421	8	50	676,650	1,323	8.1
54	0	1.41421	8	200	2,103,050	1,037	6.6
55	0	1.41421	8	200	1,801,900	1,041	6.9

generated by NR fluorescence data (0.211 and 0.265 in *R. toruloides* and *Y. lipolytica*, respectively). This implies that GC-FID as a method for lipid analysis has a limited accuracy and reliability in high-throughput contexts probably because the technical variability occuring during sample preparation and derivatization. Moreover, the adjusted high correlation coefficients (R^2) of all models (Eqs 1, 2, 3, 4, 5, and 6) being at 0.86, 0.85, and 0.85 for $Y_{1,\text{Rhoto}}$, $Y_{2,\text{Rhoto}}$, and $Y_{3,\text{Rhoto}}$, respectively, in *R. toruloides* (Table 3) and at 0.87, 0.96, and 0.818 for $Y_{1,\text{Yali}}$, $Y_{2,\text{Yali}}$, and $Y_{3,\text{Yali}}$, respectively, in *Y. lipolytica* (Table 4) indicate a strong (> 0.7) relationship between test and dependent variables, hence predictive reliability of the models.

The significance of model coefficients and the possible interaction between them was analyzed using Student *T*-test. The results showed acceptably low standard errors on the coefficients for *R. toruloides* (Table 3) and *Y. lipolytica* (Table 4) NR and GC-FID lipid titers and dry biomass models and with *t*-statistic *P*-values substantially low ($< \alpha$=0.05), indicating that the coefficients of model terms (X_1 and X_2) are statistically significant predictors of the responses (Y_1, Y_2, and Y_3) in both models. The coefficient tables (not shown) demonstrate values of the variance inflation factor (VIF), which measures how much the variance of a coefficient is inflated due to correlations across the predictors (X_1 and X_2) of the model, are all around 1 meaning that the predictors of the model are not correlated and hence that each term's coefficient is not inflated by the other terms, and thus, all model terms are well placed in the model. Overall, the coefficient tables demonstrate that, within the tested ranges of concentrations, ammonium chloride and glycerol have strong effects on lipid production in bothe yeasts. Nontheless, both ammonium chloride and glycerol have strong effects on biomass formation in *Y. lipolytica*, whereas glycerol alone has a strong effect on biomass formation in *R. toruloides*.

For both yeasts, the response surfaces were plotted as a function of ammonium chloride (X_1) and glycerol (X_2) concentrations (g/L) for lipid titers determined by NR (Y_1, RFU/L) (Fig. 5A, C), lipid titers by GC-FID (Y_2, mg/L) (Fig. 5B, D), and dry biomass response (Y_3, g/L) (Fig. 5E, F).

In both yeasts, the plots of lipid titer response (RFU/L) against ammonium chloride and glycerol concentrations (g/L) took paraboloid cylinder quadric response surfaces with steeper ascents and descents on the glycerol concentration *Z*-axis than on the ammonium chloride *X*-axis (Fig. 5A, C). This means that, at a constant ammonium chloride concentration, the lipid titers in both *R. toruloides* and *Y. lipolytica* were more sharply affected by changing the glycerol concentration than by changing the ammonium chloride concentration at a constant glycerol concentration. From an overview of the surface plots, we observe that its peak is at the middle of the tested range of glycerol concentrations and at the lowest ammonium chloride concentration (Fig. 5A, C). Interestingly, similarly to responses obtained by NR fluorescence, the plotted responses of lipid titers obtained from GC-FID (Y_2, mg/L) against ammonium chloride and glycerol concentrations (g/L) show similar elliptic paraboloid quadric response surfaces for both yeasts and similar lipid titer maxima.This similarity in lipid quantification responses between NR and GC lipid quantifications confirms the validity and reliability of our NR-based fluorometry as a method for lipid quantification (Fig. 5B, D). In addition, we emphasize again on the higher quality of lipid titer models obtained by NR-based lipid fluorometry over that obtained by GC-FID as demonstrated by the better LOF *P*-values for the former method as mentioned earlier (Tables 3 and 4). As for the dry biomass responses (g/L), the models took a nearly linear sheet for *R. toruloides* (Fig. 5E) and a cylindric paraboloid quadratic response surface for *Y. lipolytica* (Fig. 5F) where both mostly responding to changes of glycerol rather than ammonium chloride concentrations particulalry in *R. toruloides*.

The optimal values of test variables, ammonium chloride and glycerol concentration (g/L), heading for maximum lipid titers, with no constraints, were predicted from the model using the Response Optimizer function of the Minitab software (Table 5).

Table 3 Analysis of variance (ANOVA) data of the quadratic model for the test variables (Y_1, Y_2, and Y_3) as a function of ammonium chloride (X_1) and glycerol (X_2) concentrations for *R. toruloides* Y-6987

Source	Degrees of freedom	Adjusted sum of squares	Adjusted mean squares	*F*-value	*P*-value
For lipid titer ((RFU)/L) (Y_1)					
Model	4	9.47E+12	2.37E+12	46.42	0
Linear	2	4.10E+12	2.05E+12	40.15	0
X_1	1	1.55E+12	1.55E+12	30.41	0
X_2	1	2.31E+12	2.31E+12	45.21	0
Square	1	5.74E+12	5.74E+12	112.46	0
$(X_2)^2$	1	5.74E+12	5.74E+12	112.46	0
2-way Interaction	1	4.10E+11	4.10E+11	8.03	0.008
$X_1 X_2$	1	4.10E+11	4.10E+11	8.03	0.008
Error	31	1.58E+12	5.1E+10		
Lack-of-fit	4	2.98E+11	7.45E+10	1.57	0.211
Pure error	27	1.28E+12	4.75E+10		
Total	35	1.11*E*+13			
S (standard deviation) = 225,853 (RFU/L); R^2 = 0.86; R^2 (adj) = 0.84; R^2 (pred) = 0.80					
For lipid titer (mg/L) (Y_2)					
Model	3	959,400	319,800	63.58	0
Linear	2	864,575	432,288	85.94	0
X_1	1	292,250	292,250	58.10	0
X_2	1	572,325	572,325	113.78	0
Square	1	94,825	94,825	18.85	0
$(X_2)^2$	1	94,825	94,825	18.85	0
Error	35	176,050	5030		
Lack-of-fit	5	45,215	9043	2.07	0.097
Pure error	30	130,835	4361		
Total	38	1,135,450			
S (standard deviation) = 70.9 (mg/L); R^2 = 0.85; R^2 (adj) = 0.83; R^2 (pred) = 0.80					
For dry biomass (Y_3)					
Model	3	128.143	42.714	66.38	0
Linear	2	113.672	56.836	88.32	0
X_1	1	12.988	12.988	20.18	0
X_2	1	100.683	100.683	156.46	0
Square	1	14.471	14.471	22.49	0
$(X_2)^2$	1	14.471	14.471	22.49	0
Error	35	22.522	0.643		
Lack-of-fit	5	2.652	0.53	0.8	0.558
Pure error	30	19.871	0.662		
Total	38	150.665			
S (standard deviation) = 0.80 (g/L); R^2 = 0.85; R^2 (adj) = 0.84; R^2 (pred) = 0.82					

The maximum lipid titer in *R. toruloides* is 4,323,000 RFU/L which is predicted at ammonium chloride and glycerol concentrations of 4 g/L and 123 g/L, respectively, achieving a C/N molar ratio of 57 (Table 5) whereas the maximum lipid titer in *Y. lipolytica* is 3,912,000 RFU/L at ammonium chloride and glycerol concentrations of 4 g/L and 139 g/L achieving a C/N molar ratio of 61 (Table 5). Assuming that lipid titers are more reproducible when determined in cells collected from cultures with high cell densities, the model predicts the conditions achieving both maximum lipid titers and maximum biomass to be at ammonium chloride concentration of 4 g/L, for both yeasts, and at glycerol concentration of 142 g/L (C/N ratio of 66) and 136 g/L (C/N ratio of 59), for *R. toruloides* and *Y. lipolytica*, respectively. Interestingly, this is associated with lipid titers of 4,241,000 and 3,908,000 RFU/L that are lower than the values obtained when optimizing for maximal lipid titers alone by less than 2 and 0.1%, respectively (Table 5). Finally, we predicted the conditions leading to

Table 4 Analysis of variance (ANOVA) data of the quadratic model for the test variables (Y_1, Y_2, and Y_3) as a function of ammonium chloride (X_1) and glycerol (X_2) concentrations for *Y. lipolytica* W29

Source	Degrees of freedom	Adjusted sum of squares	Adjusted mean squares	*F*-value	*P*-value
For lipid titer ((RFU)/L) (Y_1)					
Model	3	4.90E+13	1.63E+13	105.3	0
Linear	2	2.11E+13	1.06E+13	68.13	0
X_1	1	1.11E+13	1.11E+13	71.48	0
X_2	1	1.00E+13	1.00E+13	64.78	0
Square	1	2.62E+13	2.62E+13	168.61	0
$(X_2)^2$	1	2.62E+13	2.62E+13	168.61	0
Error	48	7.45E+12	1.55E+11		
Lack-of-fit	5	1.01E+12	2.01E+11	1.34	0.265
Pure error	43	6.44E+12	1.50E+11		
Total	51	5.65E+13			
S (standard deviation) = 393,874 (RFU/L); $R^2 = 0.87$; R^2 (adj) = 0.86; R^2 (pred) = 0.84					
For lipid titer (mg/L) (Y_2)					
Model	5	1,002,112	200,422	155.46	0
Linear	2	236,317	118,159	91.65	0
X_1	1	71,862	71,862	55.74	0
X_2	1	168,595	168,595	130.77	0
Square	2	324,512	162,256	125.85	0
$(X_1)^2$	1	179,921	179,921	139.55	0
$(X_2)^2$	1	112,594	112,594	87.33	0
2-way interaction	1	299,429	299,429	232.25	0
$X_1 X_2$	1	299,429	299,429	232.25	0
Error	33	42,545	1289		
Lack-of-fit	2	6787	3393	2.94	0.068
Pure error	31	35,758	1153		
Total	38	1,044,657			
S (standard deviation) = 35.91 (mg/L); $R^2 = 0.96$; R^2 (adj) = 0.95; R^2 (pred) = 0.94					
For dry biomass (Y_3)					
Model	4	19.1735	4.79336	49.53	0
Linear	2	13.7643	6.88216	71.12	0
X_1	1	3.5086	3.50865	36.26	0
X_2	1	9.3541	9.35408	96.66	0
Square	1	2.8189	2.81889	29.13	0
$(X_2)^2$	1	2.8189	2.81889	29.13	0
2-Way Interaction	1	2.8537	2.85374	29.49	0
$X_1 X_2$	1	2.8537	2.85374	29.49	0
Error	45	4.3547	0.09677		
Lack-of-fit	4	0.5135	0.12837	1.37	0.261
Pure error	41	3.8413	0.09369		
Total	49	23.5282			
S (standard deviation) = 0.31 (g/L); $R^2 = 0.81$; R^2 (adj) = 0.80; R^2 (pred) = 0.77					

maximum biomass with no constraints from lipid titers and found it at ammonium chloride concentrations of 4 g/L for both yeasts and at glycerol concentrations of 191 (C/N ratio of 89) and 131 (C/N ratio of 57) g/L for *R. toruloides* and *Y. lipolytica*, respectively. In those conditions, the models predict lipid titers to be at 3,380,000 and 3,887,000 RFU/L, which is 20% and 0.6% lower than that when optimizing for maximal lipid titers alone in *R. toruloides* and *Y. lipolytica*, respectively. The settings leading to the different optimum conditions mentioned above were associated with high composite desirability (*D*) that ranged from 0.81 to 0.95, indicating that

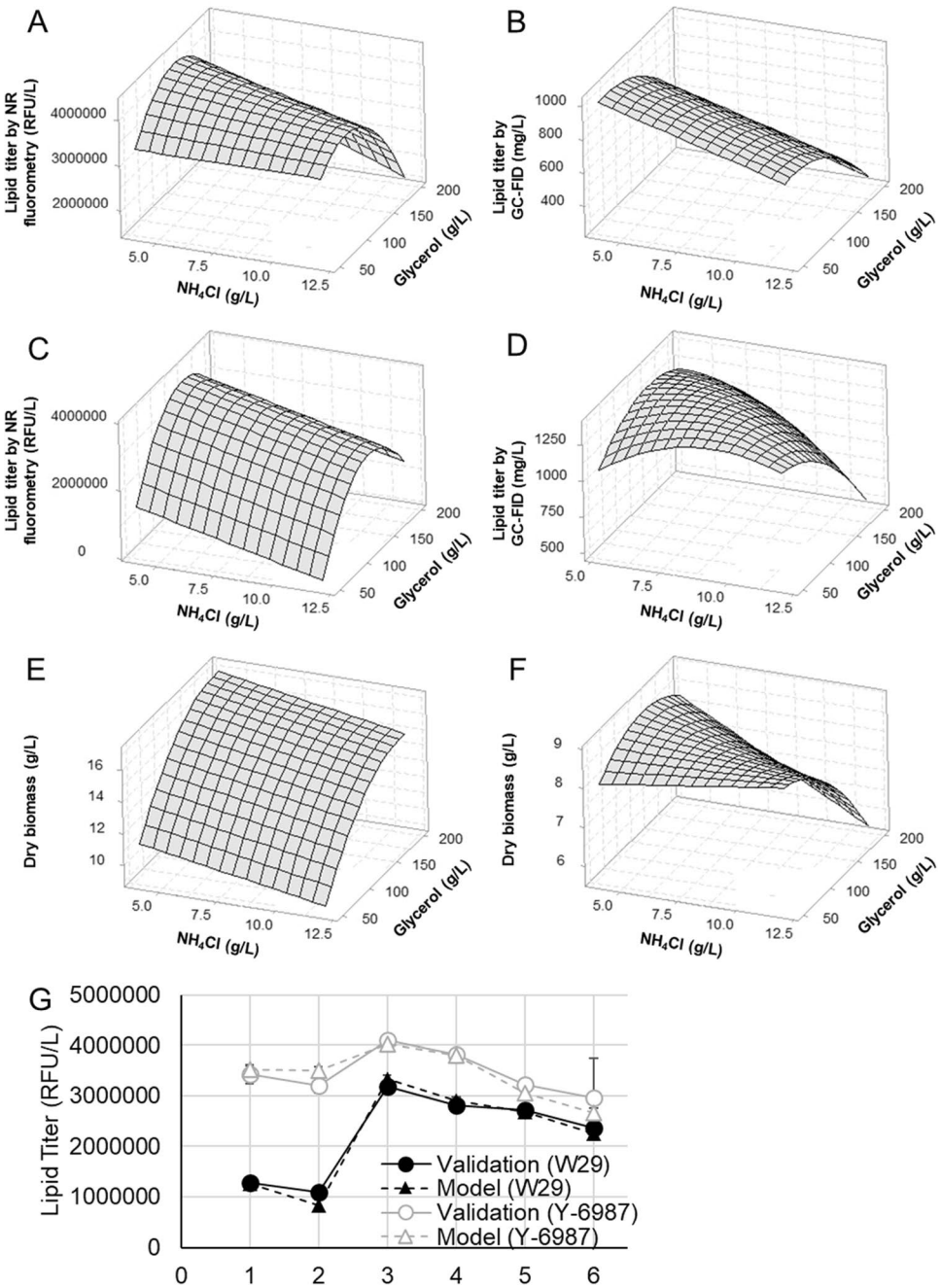

Fig. 5 Response surface and contour plots of lipid titers against ammonium chloride and glycerol concentrations in *R. toruloides* Y-6987 and *Y. lipolytica* W29. Response surface plot for **A** lipid titers estimated by NR (Y_1, RFU/L) in *R. toruloides* Y-6987 and **C** *Y. lipolytica* W29, **B** lipid titers estimated by GC-FID (Y_2, mg/L) in *R. toruloides* Y-6987 and **D**) *Y. lipolytica* W29 and **E** dry biomass (Y_3, g/L) in *R. toruloides* Y-6987 and **F** *Y. lipolytica* W29 as a function of ammonium chloride (X_1, g/L) and glycerol (X_2, g/L) concentrations according to CCD data. **G** Model validation with 6 experimentally measured arbitrary points using the NR-based fluorometry method measured in 3 biological replicates. The model points are, respectively, at ammonium chloride and glycerol concentrations of 6.8:60, 9:60, 6.8:130, 9:130, 6.8:185, and 9:185 g/L

these settings are strongly predicted to achieve favorable results towards the desired responses.

Overall, increasing the C/N ratio in *R. toruloides* from 57 to 66 decreases lipid production by only 2%; however, increasing it to 89 drastically impairs lipid production, though increasing the C/N ratios in *Y. lipolytica* from 57 to 61 does not cause a remarkable decrease in lipid production. This could entail that the optimal C/N ratio is roughly roaming around 60 for both yeasts. In consideration of C/N ratios, ratios outside of the range of 33 to 74 and of 45 to 75, respectively, in *R. toruloides* and *Y. lipolytica* are associated with a decrease of lipid production by more than 10% of maximum yields. This entails that C/N should be carefully chosen to achieve maximum lipid titers.

Finally, we validated the predictive accuracy of the models for lipid titer (Y_1, RFU/L) by measuring lipid titers at 6 arbitrary selected points with ammonium chloride concentrations of 6.8 and 9 g/L each combined with 3 glycerol concentrations of 60, 130, and 185 g/L. From the experimental lipid titers (RFU/L) plotted against the model-predicted titers, we found the absolute relative deviation to be at 6.6% from which we can conclude that the models demonstrate a high predictive accuracy (Fig. 5G).

Table 5 Optimal ammonium chloride and glycerol concentrations for maximal lipid titers in *R. toruloides* Y-6987 and *Y. lipolytica* W29 as predicted from CCD-generated model

R. toruloides Y-6987				
Dependent variables		Optimal test variables for maximum responses		
Conditions for maximum lipid titers with no constraints				
Maximum lipid titer (Y_1, RFU/L)		Ammonium chloride (X_1, g/L)	Glycerol (X_2, g/L)	C/N molar ratio
4.323E+06[a]		4	123	57
Conditions for maximum lipid titers and maximum biomass simultaneously				
Maximum lipid titer (Y_1, RFU/L)	Maximum dry biomass (Y_3, g/L)	Ammonium chloride (X_1, g/L)	Glycerol (X_2, g/L)	C/N molar ratio
4.241E+06[b]	16[b]	4	142	66
Conditions for maximum biomass with no constraints				
	Maximum dry biomass (Y_3, g/L)	Ammonium chloride (X_1, g/L)	Glycerol (X_2, g/L)	C/N molar ratio
	17[c]	4	191	89
Y. lipolytica W29				
Dependent variables		Optimal test variables for maximum responses		
Conditions for maximum lipid titers with no constraints				
Maximum lipid titer (Y_1, RFU/L)		Ammonium chloride (X_1, g/L)	Glycerol (X_2, g/L)	C/N molar ratio
3.912E+06[d]		4	139	61
Conditions for maximum lipid titers and maximum biomass simultaneously				
Maximum lipid titer (Y_1, RFU/L)	Maximum dry biomass (Y_3, g/L)	Ammonium chloride (X_1, g/L)	Glycerol (X_2, g/L)	C/N molar ratio
3.908E+06[e]	9[e]	4	136	59
Conditions for maximum biomass with no constraints				
	Maximum dry biomass (Y_3, g/L)	Ammonium chloride (X_1, g/L)	Glycerol (X_2, g/L)	C/N molar ratio
	9[f]	4	131	57

[a]The composite desirability (D) = 0.95

[b]The composite desirability (D) = 0.82

[c]The composite desirability (D) = 0.81

[d]The composite desirability (D) = 0.94

[e]The composite desirability (D) = 0.91

[f]The composite desirability (D) = 0.87

Discussion

Optimizing lipid production in oleaginous yeasts is needed to harness their full potential in the domain of oleochemical industries. The study of factors controlling lipid production requires a convenient and high-throughput lipid analysis method so that they can be tested simultaneously in a three-dimensional space using design of experiments (DoE). DoE is experimentally demanding as it requires a lot of samples (runs) to be analyzed simultaneously and in the same settings to avoid day-to-day variability, which is emphasized when working with biological systems. For example, the number of runs/samples (N) required for a simple response surface DoE involving 2 factors (k) tested at 2 levels (L) including 5 center points (c) and 4 star/axial points (s) conducted in 3 replicates (n) is equal to 39 samples as calculated from the formula $N = n\ (L^k + c + s)$. This number rapidly rises to 60 samples when adding a third factor tested at 2 levels in triplicates ($L = 2$, $k = 3$, $c = 6$, $s = 6$, $n = 3$). Again, for such type of experiments, a robust, rapid, cheap, and high-throughput protocol for lipid analysis is required, which is currently lacking and is one limiting factor preventing optimization of lipid production in oleaginous yeasts using experimentally intensive and large-scale experimental setups like DoE and large-scale screening of mutation libraries.

For such type of high-throughput experimental setups, we developed a robust Nile red-based lipid fluorometry protocol that is adapted to 96-well fluorescence microplate readers for yeasts. Using the developed protocol, 100 samples can be analyzed in less than 1 h costing less than 5 $ including the cost of Nile red (NR) dye and 96-well microplate, which is at least 50 times faster and 100 times cheaper than conventional lipid quantification methods that are based on chromatography that analyze 100 samples in at least 50 h (~ 2 sample/hour) at a total cost of as much as 500–2250$, corresponding to 10 to 45$/sample.

Nile red (NR) dye is poorly soluble (<1 µg/mL), and its fluorescence is quenched (i.e., undergo non-radiative relaxation of excited electrons to the basic state) in water, but it is very soluble and strongly fluorescent in organic solvents like acetone, ethanol, and DMSO. This dye has been successfully used to stain the core and membranes of lipid bodies by its interaction with neutral lipids (triglycerides (TG) and cholesteryl acyl esters) located in the core of this bodies as well

as with membrane phospholipids and membrane-associated hydrophobic lipoproteins (Fam et al. 2018; Greenspan and Fowler 1985). The excitation and emission wavelengths of NR range from 484 to 559 nm and 529 to 629 nm, respectively (Fam et al. 2018; Greenspan and Fowler 1985). Nonetheless, elements that affect the polarity of the intracellular environments strongly affect the NR spectral properties causing blue (by less polar metabolites like triglycerides and lipoproteins) and red (by more polar metabolites like phospholipids and cholesterols) shifts of excitation/emission ($\lambda_{em}/\lambda_{ex}$) maxima (Greenspan and Fowler 1985; Kisley 2019; Sackett and Wolff 1987). For example, $\lambda_{em}/\lambda_{ex}$ of NR are 510/585 nm in triglycerides (less polar) and 550/640 nm in phospholipids (more polar), representing a difference of maxima of 40 to 60 nm (https://www.thermofisher.com/order/fluorescence-spectraviewer/). The Filter Assistant tool of Zeiss Incorporation (https://www.micro-shop.zeiss.com/en/us/shop/filterAssistant/dyes/) recommends $\lambda_{em}/\lambda_{ex}$ of 553/636 nm for Nile red staining of lipids. In vivo however, NR fluorescence properties showed to be species-specific as they vary depending on the variable biochemical environment in every species (Rumin et al. 2015). In our study, both *Y. lipolytica* and *R. toruloides* showed optimal excitation/emission maxima at 544/678 nm, which demonstrate a red shift of emission maximum by 38 nm relative to previous reports and that might be partially attributed to a high abundance of certain polar lipids.

With respect to fluorescence intensity, it varies according to the biochemical environment where NR was reported to fluoresce intensely when bound, for example, to certain lipoproteins (Sackett and Wolff 1987). Other factors reported to affect NR fluorescence intensity include dye concentration, amount of biomass, dye permeation, staining temperature, and staining duration (Greenspan and Fowler 1985; Rumin et al. 2015). These factors were successfully optimized in this study to achieve highest fluorescence intensity.

Different final NR concentrations that ranged from 0.5 to 5 µg/mL were reported in literature (Greenspan and Fowler 1985; Kimura et al. 2004; Sitepu et al. 2012). We decided to use a NR concentration of 10 µg/mL as it was the highest possible concentration not associated with crystal formation or precipitation in a stained cell suspension when examined microscopically (data not shown).

Evidently, NR fluorescence intensity is proportional to the amount of stained oleaginous cells, yet the linear ranges of fluorescence versus cell densities showed to be species-specific (Rumin et al. 2015). For *Y. lipolytica* and *R. toruloides*, this linear range is at OD_{600} ranging from 2 to 8 and from 2 to 6, respectively, and above which the fluorescence signals plateau (Fig. 2). A similar plateau of fluorescence signal as a function of cell density was reported in the yeast, *Lipomyces starkeyi* (Kimura et al. 2004), and microalgae, *Chlorella vulgaris* (Orr and Rehmann 2015). We think that this plateau might be attributed to excessive biomaterials quenching or shielding the fluorescence signal. Although this might be species-specific, we recommend the dilution of yeast cells prior to NR staining and analysis to as close as possible to the lower limit of this linear dynamic range, which is to an OD_{600} of 2 to profit from a larger biological and instrumental dynamic range of fluorescence detection.

The NR staining temperature (Chen et al. 2009) and duration (Chen et al. 2009; Cirulis et al. 2012; Kimura et al. 2004) were reported to significantly affect fluorescence intensity in a species-specific manner. This is concordant with our findings where increasing NR staining temperature from 25 to 60 °C increased fluorescence signals by 3- to 10-folds in *Y. lipolytica* and *R. toruloides* (Fig. 3A). To the best of our knowledge, this is the first report in literature demonstrating such a significant impact on NR fluorescence intensity upon increasing incubation temperature during NR staining. A previous study demonstrated the increase of fluorescence intensity, yet by only 50% (0.5-fold), in NR staining of the microalgae, *Chlorella vulgaris*, upon increasing the staining temperature up to 50 °C (Chen et al. 2009). We suggest that increasing staining temperature assists the permeation of NR molecules into the core of lipid bodies probably by increasing the permeability of cell and lipid body membranes as well as by enhancing the solubility and retention of NR in hydrophobic lipid environment of the core of lipid bodies as previously suggested (Rumin et al. 2015). Moreover, high temperatures allow better binding of NR to certain protein or lipoproteins by changing the conformation of certain proteins exposing more their hydrophobic regions for a better interaction with NR leading to an increase in the dye's fluorescence intensity (Sackett and Wolff 1987). We think that using high temperatures during NR staining might overcome any differential cell uptake of NR dye that might occur at different phases of cell growth thus making staining procedure more reproducible across different cell viability states.

Increasing staining durations to 30 min resulted in 2- to 3-fold increase of fluorescence intensity relative to an incubation of 5 min (Fig. 3B) which corroborates with previous reports that showed a higher NR fluorescence intensity after 20–30 min of NR staining in oleaginous yeasts (Ramírez-Castrillón et al. 2021). There is not, however, a universal duration for NR staining as it seems also species-specific (Rumin et al. 2015), and thus, we recommend that it be optimized for each microorganism individually.

It is worthy to mention that lipid bodies of cells stained according to our protocol, 10 µg/L NR at 60 °C for 30 min, were amazingly resistant to photobleaching during examination using fluorescence microscopy (data not shown). Photobleaching is the loss of fluorescence upon exposure to light that is commonly encountered in fluorescence microscopy of NR-red stained lipid bodies (Lamprecht and Benoit 2003). This is caused by light-mediated photolysis of the

fluorophore or, more importantly, by a non-specific photochemical reaction of the fluorophore with surrounding hydrophilic molecules (Ray et al. 2019). Some reports demonstrated that NR suffers photobleaching only in aqueous environments and not in organic solvents (Ray et al. 2019). Therefore, we suggest that the resistance to photobleaching observed in our staining protocol, is particularly attributed to the use of 60°C staining temperature, which allows more NR to permeate and be retained into the lipid environment of the inner core of lipid bodies, where it becomes more protected from the non-specific photochemical reactions with the hydrophilic molecules in the aqueous cytosol.

Using our protocol, we developed an arbitrary scale for determination of lipogenicity of microorganism according to which a microorganism might be classified as lipogenic (oleaginous) only if its specific fluorescence is 3 times that of a non-lipogenic bacteria, *E. coli*, or 2 times that of a non-lipogenic yeasts, like *S. cerevisiae* (Fig. 3C). It should be mentioned however that *S. cerevisiae* shifts to fermentative metabolism under the nitrogen-limited condition of cultivation used in this study and which induces the production of ethanol (Tesnière et al. 2015), which might boost NR fluorescence intensity, the fact that might decreased our cutoff of lipogenecity when normalizing to non-lipogenic yeasts. Nonetheless, our protocol remains useful for large-scale screening of potential oleaginous organisms using whichever cutoffs.

Using the NR-based lipid fluorometry, we compared lipid titers (RFU/L) and specific lipid productivity (RFU/g biomass) of *Y. lipolytica* and *R. toruloides* across the growth curve. We show that both species had similar specific lipid productivity, peaking on the 3rd day for both yeasts, and similar net lipid titers peaking on the 3rd day and 8th day for *Y. lipolytica* and *R. toruloides*, respectively (Fig. 4). The oleaginous yeasts, *R. toruloides* and *Y. lipolytica*, have been previously reported to naturally accumulate lipids at 70% and 40% of their dry cell weight, yet using non-specific gravimetric lipid quantitation methods (Nicaud 2012; Ratledge and Wynn 2002). We report however that *R. toruloides* and *Y. lipolytica* accumulate lipids at about 10% and 20% of their dry cell weight, respectively. We believe that our NR fluorescence data that were calibrated by GC-FID analysis are far more specific and reliable than gravimetric lipid determination currently used in literature as the latter is less specific and more prone to errors. Noteworthy, the optimal conditions identified in this study were for the best lipid content per unit volume of culture after 3 days of cultivation which is not necessarily the optimal conditions for highest lipid content per unit biomass. In that regard, even though *R. toruloides* accumulated lower amount of lipids per unit biomass, this is compensated by its higher growth achieving a higher overall lipid content per unit volume of culture.

There have been many attempts in literature to calibrate NR-based fluorescence values into actual lipid quantities, one of which is by using triolein as standard lipid. Nonetheless, this approach suffers two limitations. First, triolein has a very narrow linear range from 0.5 to 25 µg/L (Poli et al. 2014). Second, triolein solutions are usually prepared in isopropanol or hexane in which NR has already an intense background fluorescence that masks the weak signal emitted from triolein itself (Isleten-Hosoglu et al. 2012). Probably, triolein oil-in-water emulsions using emulsifiers like lecithin might remediate this problem. We succeeded however to make such calibration using GC-FID (Fig. 4C) in which 400,000 RFU/L corresponds to 350 and 70 mg/L of lipids, respectively, in *R. toruloides* and *Y. lipolytica*. It should be noted however that new calibration curves should regularly be made with fresh NR solution (not older than 1 month) that will be used for NR-based lipid fluorometry in standard and test samples to avoid RFU variations resulting from changes in NR concentration caused by the evaporation of its solvent, acetone. Moreover, we believe that optimization of staining conditions should be made specifically for every new microbial strain and that regression equations from calibration curves obtained for specific strains should not be universally applied across different microbial strains or even for the same strain across different experimental setups. This is because strain-dependent variations in lipid content could be observed across different strains of the same lipogenic yeast species as previously reported (Miranda et al. 2020).

The developed NR-based lipid fluorometry demonstrated to be efficient and convenient lipid quantitation method in the optimization of concentrations of nitrogen and carbon sources using full factorial central composite design (CCD) (Eqs. 1 and 4). This demonstrated the strong (> 0.7) regression coefficients (adjusted $R^2 = 0.84$ and 0.86) of generated models (Tables 3 and 4). To boost the regression coefficient to values closer to 1, further improvements in NR-based lipid fluorometry could be introduced aims at decreasing technical variation and hence the standard deviation of the method.

Results of response surfaces of CCD show that the optimal points for maximal lipid production in *R. toruloides* are at ammonium chloride and glycerol concentrations of 4 and 123 g/L, respectively, which achieves a molar C/N ratio of 57 (Table 5). This is close to the optimal points for maximal lipid production in *Y. lipolytica* that are at 4 and 139 g/L achieving a molar C/N ratio of 61 (Table 5). Different optimal C/N were reported in literature for oleaginous yeasts ranging from more than 20 (Abdel-Mawgoud et al. 2018; Hildyard and Halestrap 2003; Nielsen 2014; Papanikolaou and Aggelis 2011b; Ratledge 1997; Ratledge and Wynn 2002) up to 100 (Kuttiraja et al. 2016). The latter study investigated, however, C/N of 25, 50, 100, and 150 in *Y. lipolytica* (Kuttiraja et al. 2016) that overlooked C/N

between 50 and 100; thus, our optimal C/N of 61 for this yeast is seemingly a refined measurement of the optimal C/N for highest lipid accumulation. We observed that increasing the C/N ratio above the optimal value is associated with a decrease in lipid production; this was also reported in *R. toruloides* (Moreton 1988; Papanikolaou and Aggelis 2011b).

In conclusion, we present an optimized Nile red-based lipid fluorometry protocol that supported a high-throughput experiment like the optimization of medium components using full factorial response surface central composite design (CCD). The developed protocol is cheap, rapid, reliable, and high throughput. It is thus suitable for large-scale experiments requiring the analysis of large number of samples, like CCD, screening for oleaginous organisms, genome wide screening of genetic regulators of lipid production and for various synthetic biology purposes. This study also reports the optimum concentrations of ammonium chloride and glycerol as well as the molar C/N ratio for maximum lipid production in *Rhodotorula toruloides* Y-6987 and *Yarrowia lipolytica* W29.

Supplementary Information The online version contains supplementary material available at https://doi.org/10.1007/s00253-023-12786-9.

Author contributions BO and ZM were students in AMAM's lab and equally contributed to conducting the experiments under his supervision, including culturing, sample collection and analysis, data processing, statistical analyses, and data visualization, and wrote the draft of the manuscript. AMAM conceived the work plan, supervised the research work, analyzed data wrote and edited the manuscript, and provided funding and resources. All authors read and approved the manuscript.

Funding This work was funded by NSERC-Discovery Grant (RGPIN-2022-05307) and Fonds de recherche du Québec–Nature et technologies (FRQNT)-Établissement de la Relève Professorale (application no. 2022-NC-298442), to Professor Ahmad M. Abdel-Mawgoud. Mr. Benjamin Ouellet was a MSc student and was funded by Fonds de recherche du Québec–Nature et technologies (FRQNT)-MSc scholarship. Mr. Zacharie Morneau was a student funded by NSERC-USRA, Canada.

Data availability All data generated or analyzed during this study are included in this published article.

Declarations

Ethics approval This article does not contain any studies with human participants or animals performed by any of the authors.

Competing interests The authors declare no competing interests.

References

Abdel-Mawgoud AM, Markham KA, Palmer CM, Liu N, Stephanopoulos G, Alper HS (2018) Metabolic engineering in the host *Yarrowia lipolytica*. Metab Eng 50:192–208. https://doi.org/10.1016/j.ymben.2018.07.016

Abdel-Mawgoud AM, Stephanopoulos G (2020) Improving CRISPR/Cas9-mediated genome editing efficiency in *Yarrowia lipolytica* using direct tRNA-sgRNA fusions. Metab Eng 62:106–115. https://doi.org/10.1016/j.ymben.2020.07.008

Blazeck J, Hill A, Liu L, Knight R, Miller J, Pan A, Otoupal P, Alper HS (2014) Harnessing *Yarrowia lipolytica* lipogenesis to create a platform for lipid and biofuel production. Nat Commun 5(1):3131. https://doi.org/10.1038/ncomms4131

Chen W, Zhang C, Song L, Sommerfeld M, Hu Q (2009) A high throughput Nile red method for quantitative measurement of neutral lipids in microalgae. J of Microbiol Methods 77(1):41–47. https://doi.org/10.1016/j.mimet.2009.01.001

Cirulis JT, Strasser BC, Scott JA, Ross GM (2012) Optimization of staining conditions for microalgae with three lipophilic dyes to reduce precipitation and fluorescence variability. Cytomet Part A 81A(7):618–626. https://doi.org/10.1002/cyto.a.22066

da Silva GP, Mack M, Contiero J (2009) Glycerol: a promising and abundant carbon source for industrial microbiology. Biotechnol Advanc 27(1):30–39. https://doi.org/10.1016/j.biotechadv.2008.07.006

Dobrowolski A, Drzymala K, Rzechonek DA, Mitula P, Mironczuk AM (2019) Lipid production from waste materials in seawater-based medium by the yeast *Yarrowia lipolytica*. Front in Microbiol 10:9. https://doi.org/10.3389/fmicb.2019.00547

Fam TK, Klymchenko AS, Collot M (2018) Recent advances in fluorescent probes for lipid droplets. Mater 11(9):1768

Greenspan P, Fowler SD (1985) Spectrofluorometric studies of the lipid probe, Nile red. J of Lipid Res 26(7):781–789. https://doi.org/10.1016/S0022-2275(20)34307-8

Henne WM, Reese ML, Goodman JM (2018) The assembly of lipid droplets and their roles in challenged cells. EMBO J 37(12). https://doi.org/10.15252/embj.201898947

Hildyard JCW, Halestrap AP (2003) Identification of the mitochondrial pyruvate carrier in *Saccharomyces cerevisiae*. Biochem J 374(3):607–611. https://doi.org/10.1042/bj20030995

Isleten-Hosoglu M, Gultepe I, Elibol M (2012) Optimization of carbon and nitrogen sources for biomass and lipid production by *Chlorella saccharophila* under heterotrophic conditions and development of Nile red fluorescence based method for quantification of its neutral lipid content. Biochem Eng J 61:11–19. https://doi.org/10.1016/j.bej.2011.12.001

Johns AMB, Love J, Aves SJ (2016) Four inducible promoters for controlled gene expression in the oleaginous yeast *Rhodotorula toruloides*. Front in Microbiol 7(1666). https://doi.org/10.3389/fmicb.2016.01666

Kimura K, Yamaoka M, Kamisaka Y (2004) Rapid estimation of lipids in oleaginous fungi and yeasts using Nile red fluorescence. J of Microbiol Methods 56(3):331–338. https://doi.org/10.1016/j.mimet.2003.10.018

Kisley L (2019) Chapter 3 - Single molecule spectroscopy at interfaces. In: Johnson CK (ed) Spectroscopy and dynamics of single molecules. Elsevier, pp 117–161

Kitcha S, Cheirsilp B (2011) Screening of oleaginous yeasts and optimization for lipid production using crude glycerol as a carbon source. Energy Procedia 9:274–282. https://doi.org/10.1016/j.egypro.2011.09.029

Kuttiraja M, Douha A, Valéro JR, Tyagi RD (2016) Elucidating the effect of glycerol concentration and C/N ratio on lipid production using *Yarrowia lipolytica* SKY7. Appl Biochem and Biotechnol 180(8):1586–1600. https://doi.org/10.1007/s12010-016-2189-2

Lamprecht A, Benoit J-P (2003) Simple liquid-chromatographic method for Nile red quantification in cell culture in spite of photobleaching. J Chromatogr B 787(2):415–419. https://doi.org/10.1016/S1570-0232(02)00962-5

Miranda C, Bettencourt S, Pozdniakova T, Pereira J, Sampaio P, Franco-Duarte R, Pais C (2020) Modified high-throughput Nile red fluorescence assay for the rapid screening of oleaginous yeasts

using acetic acid as carbon source. BMC Microbiol 20(1):60. https://doi.org/10.1186/s12866-020-01742-6

Moreton R (1988) Single cell oil. Longman Scientific Technical, Harlow

Nicaud JM (2012) *Yarrowia lipolytica*. Yeast 29(10):409–418. https://doi.org/10.1002/yea.2921

Nielsen J (2014) Synthetic biology for engineering acetyl coenzyme A metabolism in yeast. mBio 5(6):e02153–e02114. https://doi.org/10.1128/mBio.02153-14

Orr V, Rehmann L (2015) Improvement of the Nile red fluorescence assay for determination of total lipid content in microalgae independent of chlorophyll content. J of Appl Phycol 27(6):2181–2189. https://doi.org/10.1007/s10811-014-0481-5

Papanikolaou S, Aggelis G (2011a) Lipids of oleaginous yeasts. Part I: Biochemistry of single cell oil production. Eur J Lipid Sci Technol 113(8):1031–1051. https://doi.org/10.1002/ejlt.201100014

Papanikolaou S, Aggelis G (2011b) Lipids of oleaginous yeasts. Part II: Technology and potential applications. Eur J Lipid Sci Technol 113(8):1052–1073. https://doi.org/10.1002/ejlt.201100015

Poli JS, Lützhøft H-CH, Karakashev DB, Valente P, Angelidaki I (2014) An environmentally-friendly fluorescent method for quantification of lipid contents in yeast. Bioresour Technol 151:388–391. https://doi.org/10.1016/j.biortech.2013.09.128

Pomraning KR, Wei S, Karagiosis SA, Kim Y-M, Dohnalkova AC, Arey BW, Bredeweg EL, Orr G, Metz TO, Baker SE (2015) Comprehensive metabolomic, lipidomic and microscopic profiling of *Yarrowia lipolytica* during lipid accumulation identifies targets for increased lipogenesis. Plos One 10(4):e0123188. https://doi.org/10.1371/journal.pone.0123188

Ouellet B, Abdel-Mawgoud AM (2023) Strong Expression of Cas9 Under a New 3'-Truncated TEF1α Promoter Enhances CRISPR-Cas9-Mediated Genome Editing in Yarrowia Lipolytica. Yarrowia Lipolytica. https://doi.org/10.2139/ssrn.4499951

Quispe CAG, Coronado CJR, Carvalho JA Jr (2013) Glycerol: production, consumption, prices, characterization and new trends in combustion. Renew Sustain Energy Rev 27:475–493. https://doi.org/10.1016/j.rser.2013.06.017

Ramírez-Castrillón M, Jaramillo-Garcia VP, Lopes Barros H, Pegas Henriques JA, Stefani V, Valente P (2021) Nile red incubation time before reading fluorescence greatly influences the yeast neutral lipids quantification. Front Microbiol 12(445). https://doi.org/10.3389/fmicb.2021.619313

Ratledge C (1997) Microbial Lipids. Biotechnol:133–197

Ratledge C, Wynn JP (2002) The biochemistry and molecular biology of lipid accumulation in oleaginous microorganisms. Advanc Appl Microbiol 51:1–51. https://doi.org/10.1016/s0065-2164(02)51000-5

Ray A, Das S, Chattopadhyay N (2019) Aggregation of Nile red in water: prevention through encapsulation in β-cyclodextrin. ACS Omega 4(1):15–24. https://doi.org/10.1021/acsomega.8b02503

Rumin J, Bonnefond H, Saint-Jean B, Rouxel C, Sciandra A, Bernard O, Cadoret J-P, Bougaran G (2015) The use of fluorescent Nile red and BODIPY for lipid measurement in microalgae. Biotechnol Biofuels 8(1):42. https://doi.org/10.1186/s13068-015-0220-4

Sackett DL, Wolff J (1987) Nile red as a polarity-sensitive fluorescent probe of hydrophobic protein surfaces. Anal Biochem 167(2):228–234. https://doi.org/10.1016/0003-2697(87)90157-6

Sitepu IR, Ignatia L, Franz AK, Wong DM, Faulina SA, Tsui M, Kanti A, Boundy-Mills K (2012) An improved high-throughput Nile red fluorescence assay for estimating intracellular lipids in a variety of yeast species. J Microbiol Methods 91(2):321–328. https://doi.org/10.1016/j.mimet.2012.09.001

Tesnière C, Brice C, Blondin B (2015) Responses of *Saccharomyces cerevisiae* to nitrogen starvation in wine alcoholic fermentation. Appl Microbiol Biotechnol 99(17):7025–7034. https://doi.org/10.1007/s00253-015-6810-z

Van Wychen S, Ramirez K, Laurens LML (2016) Determination of total lipids as fatty acid methyl esters (FAME) by *in situ* transesterification: laboratory analytical procedure (LAP). Natl Renew Energy Lab: Tech Rep(NREL/TP-5100-60958). https://doi.org/10.2172/1118085

Zhang HY, Wu C, Wu QY, Dai JB, Song YD (2016) Metabolic flux analysis of lipid biosynthesis in the yeast *Yarrowia lipolytica* using C-13-labled glucose and gas chromatography-mass spectrometry. Plos One 11(7):14. https://doi.org/10.1371/journal.pone.0159187